

## Determination of AC test currents for thermo-electric laboratory stresses on gas-insulated HVDC systems

M. HALLAS<sup>1</sup>, M. KOSSE<sup>2</sup>, K. JUHRE<sup>2</sup>, M. SECKLEHNER<sup>3</sup>, V. HINRICHSEN<sup>1</sup>

<sup>1</sup>Technical University of Darmstadt, Germany

<sup>2</sup>Siemens Energy, Germany

<sup>3</sup>Baur, Austria

### SUMMARY

A particular challenge in the design of HVDC equipment is the accumulation of electrical charge carriers at gas-solid interfaces and in the bulk of the solid insulation material, which can cause locally increased electrical field stress. During operation, a current flows through the conductor, leading to an inhomogeneous temperature distribution between conductor and enclosure. Thus, the solid epoxy insulators are experiencing the whole temperature gradient. As the electric field distribution at DC voltage is mainly determined by the conductivities of the applied insulating media and the conductivity of epoxy resin is strongly temperature-dependent, the temperature distribution has a major impact on the electric field distribution and with this on the dielectric performance of the insulation system. Hence, testing of gas-insulated HVDC equipment always requires the consideration of high current and high DC voltage at the same time. An AC test current is typically used to generate the temperature gradient in the insulating system. However, the commercial operation of the HVDC equipment with DC current must be reflected, when thermo-electric tests in the laboratory are performed with AC current.

This paper presents temperature-rise tests with different AC and DC test currents up to 5000 A, applied to commercial gas-insulated HVDC equipment. Based on the test data, different approaches for the determination of representative test currents for thermo-electric tests are discussed. In conclusion, a representative AC test current for the given HVDC equipment is proposed, which considers all major effects for thermo-electric testing. To reduce the practical efforts for future laboratory tests, the calculation approach for AC test currents of HVDC bushings (IEC/IEEE 65700-19-03) is evaluated with regard to a possible application to the tested gas-insulated HVDC equipment. The result is compared with the measured data. The paper shows the application of this standard to gas-insulated systems and proposes further possible optimizations.

### KEYWORDS

Thermo-electric tests, gas-insulated HVDC equipment, temperature-rise test, AC current heating, DC current heating, DC GIS, DC gas-insulated switchgear assemblies

## 1. INTRODUCTION

The design of gas-insulated HVDC equipment has to consider specific DC effects, especially charge accumulation at the surface and in the bulk of solid insulating materials. Furthermore, the temperature dependence of the materials' electrical resistance, which considerably influences the electric field distribution of the gas-solid insulation system under typical service conditions with a temperature gradient along the insulation has to be taken into account. Hence, recommendations of CIGRE JWG D1/B3.57 for gas-insulated HVDC equipment propose a thermo-electric test – the so-called *insulation system test*.<sup>1</sup> Aim of this test is to verify the dielectric behavior of the gas-insulated system under high load conditions, i.e. with a continuous heating period at rated current up to the thermal steady state. The used heating method shall be conductor heating, reaching the maximum conductor temperature and maximum temperature gradient across the insulation. [1]

In principle, three current heating options are possible to fulfill the CIGRE JWG's requirements [2]:

- Option (1) AC current heating (r.m.s. value) with rated DC current value
- Option (2) AC current heating with representative AC current (r.m.s. value)
- Option (3) DC current heating with rated current

According to option 1, equipment with a rated DC current for example of  $I_{rDC} = 5000$  A would be tested with  $I_{AC} = 5000$  A (r.m.s. value) in the laboratory. This option will safely cover the later operation, but will also result in higher thermal stresses, since the skin effect at AC current increases the power losses in the assembly. Thermo-electric stresses due to different charge formation will thereby be higher in the laboratory compared to the regular operation in the grid.

Option 3 will test the HVDC equipment according to the later operation in the grid without any further calculation methods. It requires the injection of DC current at DC voltage magnitudes. Generators to inject high DC current at high voltage potential are still under research [2]. High voltage laboratories therefore typically apply AC current heating, since standard encapsulated AC current transformers can easily be used to inject the current in a loop formed by the inner conductor.

For option 2, an AC test current (r.m.s. value)  $I_{AC\ repr.}$  has to be determined, which is representative for the later DC operation in the grid. Calculations and comparisons between DC and AC current temperature-rise tests are required to justify equal or higher stresses at the equipment than with the rated DC current  $I_{rDC}$ . This paper aims to present methods for determining this representative AC test current  $I_{AC\ repr.}$

## 2. THERMO-ELECTRIC BEHAVIOUR OF GAS-INSULATED SYSTEMS

For AC current heating with  $I_{AC\ repr.}$ , the current has to be adjusted in order to reach equivalent or higher thermal stress compared to the stress resulting from DC current application. It has to be investigated, how this requirement can be fulfilled for practical arrangements and which parameters have to be compared for AC and DC current heating. Therefore, a comprehensive understanding of the thermo-electric behavior of gas-insulated HVDC systems is required to find a representative AC test current for the operation in the grid.

The electric field distribution under DC voltage stress is influenced by several parameters, such as temperature, electric field strength, charge accumulation, humidity. The conductor current mainly influences the temperature distribution and with this the electric field distribution under DC voltage stress, since for most of the insulating materials the specific electric conductivity  $\kappa$  depends on the absolute temperature  $T$  [3] (Figure 1). Shortly after energizing with DC voltage, the electric field distribution is determined by the electric permittivities and is therefore equal to the capacitive AC field distribution. Since the permittivity is virtually independent of the temperature, the status in Figure 1 (a) is independent of the current stress. During continuous DC voltage stress, the capacitive field distribution evolves with time into a resistive field distribution, reaching 90% of this state after time  $t_{90}$ , which is according to CIGRE JWG D1/B3.57 defined as *DC steady state* [1]. The electric conductivity of the insulation material becomes of major influence. Without current  $I$  through the inner conductor, the maximum electric field stress appears close to the inner conductor, because the conductivity across the solid insulation stays mainly homogeneous (Figure 1 (b)). By applying a current  $I$  to the inner

---

<sup>1</sup> CIGRE JWG D1/B3.57 furthermore introduces a *prototype installation test* with a test duration of one year. This test also demands high load cycles to test the thermo-electric behaviour during long-term operation. The determination of an AC test current is of interest for this test as well.

conductor, the conductivity of the solid insulator close to the heated inner conductor is much higher than at the colder enclosure. This may lead to a “field-inversion” due to charge accumulation, where the maximum electrical field strength is shifted towards the enclosure (Figure 1 (c)) [4], [5], [6], [7], [8]. The results in Figure 1 show the high influence of the current  $I$  and the resulting temperature distribution in the insulating material on the electric field distribution [9]. In conclusion, a field transition takes place from the electrostatic field (Figure 1 (a)) to the quasi-stationary electric flow field (Figure 1 (c)) due to the resulting temperature gradient by applying a current  $I$ . This process takes usually days to weeks [1].<sup>2</sup> Literature describes more influencing parameters, such as contact phenomena at the electrodes [10], [11], or additional space charges [12], which are neglected in this paper.

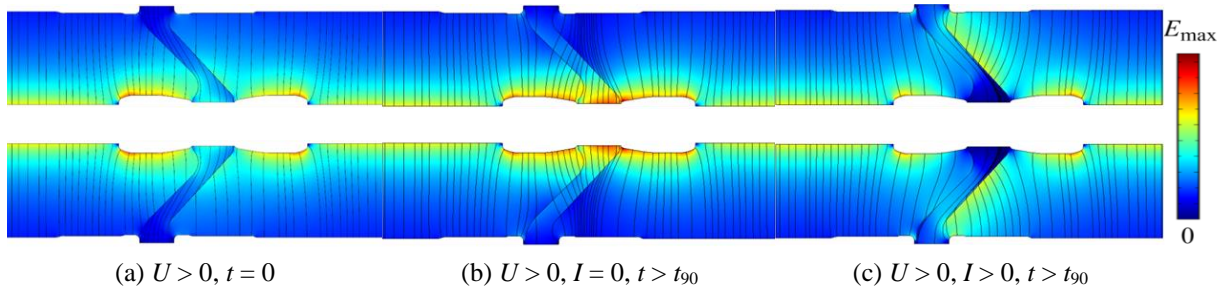


**Figure 1:** Calculated electric field distribution of a coaxial gas-insulated system under DC voltage stress at different times after energization with and without a conductor current [9]

For HVDC applications, the insulators are components of high relevance during thermo-electric testing [1], [13]. Their electric field distribution mainly depends on the temperature gradient  $\Delta T$  between inner conductor and enclosure (refer Figure 1). Hence,  $I_{AC\ repr.}$  has to be adjusted to the  $\Delta T$  at the insulators resulting from  $I_{r\ DC}$ .

Despite the fact that the electric conductivity changes by orders of magnitude with the absolute temperature [3], the absolute temperature for technical application is often of minor importance. As long as the temperature gradient stays the same, basically the transition time from capacitive to resistive field is decreased by increasing absolute temperature [5]. The electric field distribution, e.g. in Figure 1 (c) would not change significantly in the range of relevant ambient temperatures.

The temperature dependence of the insulating gas conductivity is often neglected and assumed to be constant, since it is relatively low compared to commonly used solid insulation materials [1]. Therefore, its influence on the field transition is neglectable. But since the withstand voltage is depending on the gas pressure and with this on the gas density, a locally decreased gas density due to gas convection close to the conductor may lead to a decreased withstand voltage. This mechanism is triggered by the maximum temperature rise  $\theta$  at the inner conductor [14], [15].

In conclusion, an equivalent AC test current has to deliver similar temperature gradients  $\Delta T$  at the insulators as well as temperature rises  $\theta$  at the inner conductor. For  $I_{AC\ repr.}$ , the values of  $\Delta T$  and  $\theta$  at all sensor positions should be at least equivalent or higher than for  $I_{r\ DC}$ . Hence, with respect to CIGRE JWG D1/B3.57, the following two requirements have to be fulfilled:

$$\text{Definition (1)} \quad \Delta T(I_{AC\ repr.}) \geq \Delta T(I_{r\ DC})$$

$$\text{Definition (2)} \quad \theta(I_{AC\ repr.}) \geq \theta(I_{r\ DC})$$

### 3. DETERMINATION OF A REPRESENTATIVE AC TEST CURRENT

Temperature-rise and temperature gradient within the gas-insulated system under DC current have to be compared with that one under AC current to determine the test current for thermo-electric testing. Gas-insulated systems, such as gas-insulated switchgears (GIS) and lines (GIL), are composed of several different modules, such as disconnecter, X-, T- or angle-modules. Each module has a different shape and thereby different thermal properties. This also leads to different temperature rise values  $\theta$ , as well as gradients  $\Delta T$ , resulting in different electric field distributions for each module. Nevertheless, the AC test current has to be valid for each module. This requirement has to be investigated by comparing the

<sup>2</sup> The thermal heating process does not influence the DC transition process very much, since this process takes only some hours and is assumed to be faster than the charge accumulation.

resulting temperature-rise and gradient of the different modules at AC and DC current. A valid test current for all gas compartments is thereby determined. For this purpose, a temperature-rise test assembly was built up with all major HVDC GIS modules. Figure 2 shows the test assembly.

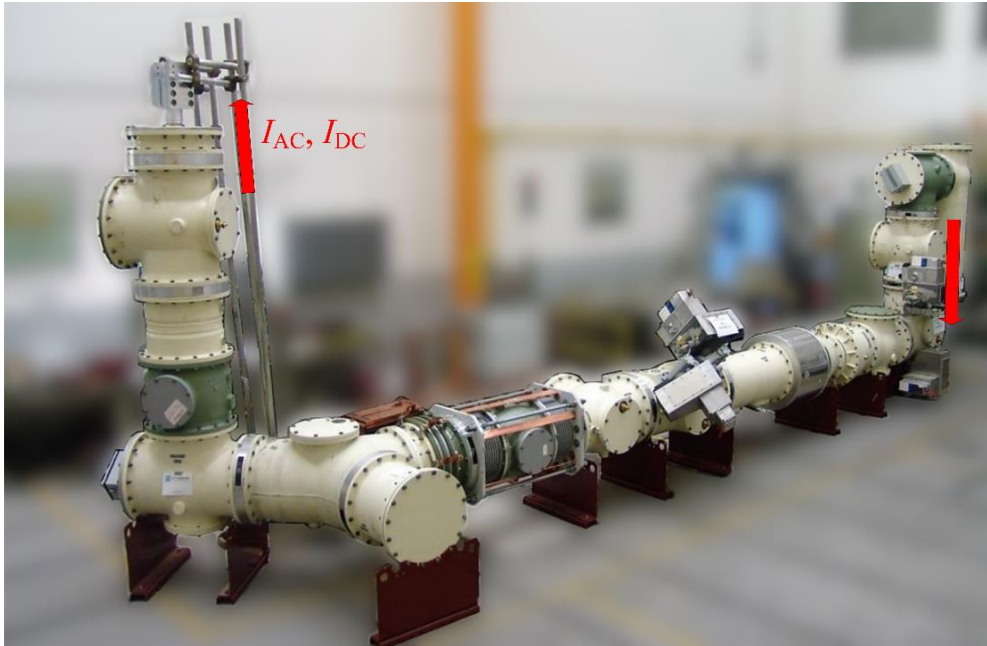


**Figure 2:** Temperature-rise test assembly for AC and DC current heating

In total 11 gas compartments were investigated with 90 thermal sensors at the inner conductor and 23 sensors at the enclosure. As it is common for AC GIS, the sensors were placed at potential hot spots close to electrical contacts within the inner conductor line. Within the 90 sensors, 18 sensor positions were close to both sides of 9 insulators. The sensors at the enclosure were placed at the insulators and in the middle of the compartments, since the temperature at the solid alloy enclosure is distributed very homogeneously. The temperature-rise test was performed in accordance with IEC 62271-203 [16]. The rated current and voltage values of the HVDC GIS are 5000 A DC and  $\pm 550$  kV DC respectively.

### 3.1. TEST RESULTS

The test assembly was stressed with 2500 A, 3150 A, 4000 A and 5000 A AC (r.m.s. values) as well as DC. The results for all 113 sensor positions are given in Figure 3. The temperature-rise  $\theta$  represents the difference of the measured temperature to the ambient temperature. The temperature gradient  $\Delta T$  is defined as the difference between inner conductor and enclosure. The temperature gradient  $\Delta T$  across the insulator and the gas gap are determined by using the  $\theta$  values of the respective sensors at the inner conductor and the enclosure. To determine  $\Delta T$  for the gas gap, all conductor sensors in one compartment are assigned to the single respective sensor of the enclosure. The values of  $\theta$ , as well as  $\Delta T$ , are normalized to the hot-spot temperature-rise at 5000 A DC.

As expected, the AC currents result generally in higher temperature rises  $\theta$  and gradients  $\Delta T$  than for the DC currents. Compared to 5000 A DC, the 5000 A AC data results in (12...26) % higher  $\theta$  at the conductor (Figure 3 (a) and (b)) and (6...15) % higher  $\theta$  at the enclosure (Figure 3 (c)) and (d)). The values of  $\Delta T$  at the insulators differ from 6 % to 12 % (Figure 3 (e)) and (f)) and across the gas gap in the range of (3...13) % (Figure 3 (g)) and (h)). This means that option 1 according to section 1 would result in higher thermal and thereby also thermo-electric stresses compared to DC heating. Hence, option 1 would stress the equipment during thermo-electric testing more than during operation.

The temperature-rise  $\theta$  at the inner conductor significantly differs at the different positions due to the different electrical contact properties. The differences in the temperature-rise  $\theta$  at the enclosure are moderate and, as expected, not so much differing for the different positions. The highest temperature occurs at an enclosure with lower wall thickness.

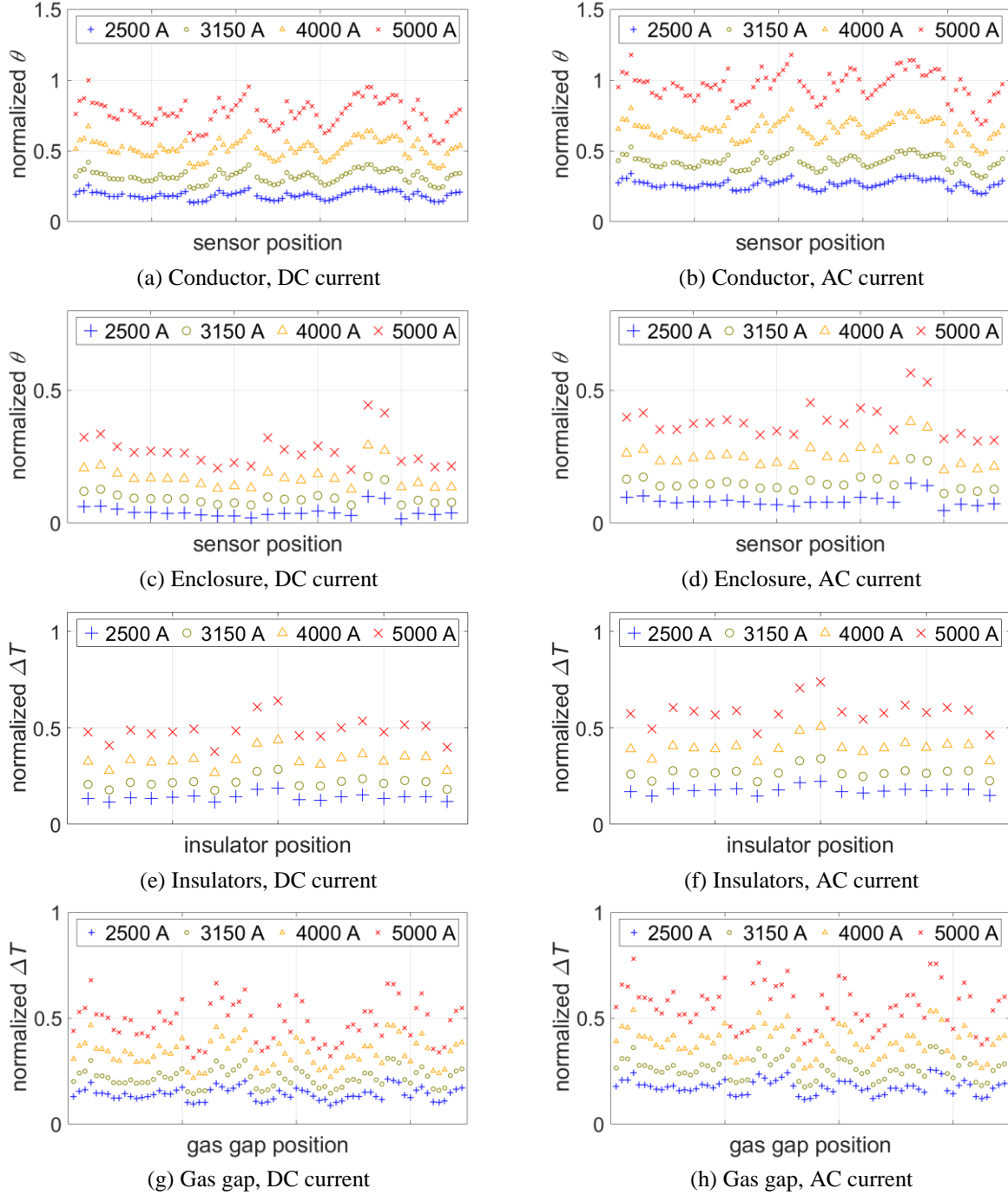


**Figure 3:** Normalized temperature rises  $\theta$  and temperature gradients  $\Delta T$  at the HVDC GIS components for AC and DC current stresses

### 3.2. TEST CURRENT CALCULATION FOR $\Delta T$ ACROSS THE INSULATORS

In order to determine the representative AC test current  $I_{AC\text{ repr.}}$  for a rated DC current  $I_{r\text{ DC}}$  based on the relevant temperature gradient  $\Delta T$ , an interpolated data curve  $\Delta T_{\text{interpol}} = f(I_{AC})$  can be utilized. To fulfill the minimum requirements of CIGRE JWG D1/B3.57, the interpolation curve has to reassure that each  $\Delta T$  of  $\Delta T_{\text{interpol}}$  is at least equal to the  $\Delta T$  of the respective rated DC current. The following relation has to be fulfilled for each position:  $\Delta T_{\text{interpol}}(I_{AC\text{ repr.}}) \geq \Delta T(I_{r\text{ DC}})$ .

For example, in Figure 3 (f), a test current between 4000 A AC and 5000 A AC has to be found, that leads to at least the same  $\Delta T$  as in Figure 3 (e) corresponding to 5000 A DC, named  $\Delta T(5000\text{ A DC})$ . Hence, for each  $\Delta T_i$  at sensor point  $i$ , an interpolated data curve  $\Delta T_{i,\text{interpol}}(I_{AC})$  is determined by taking into account all measurement data. A cubic spline interpolation is used to get  $\Delta T_{i,\text{interpol}}(I_{AC})$ . Figure 4

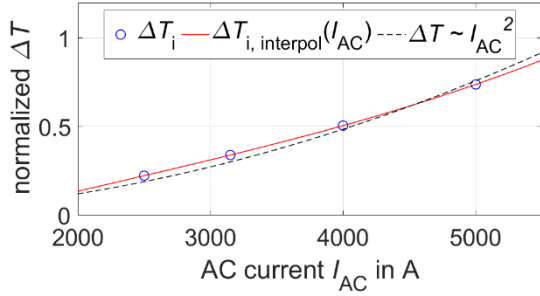


**Figure 4:** Determination of the interpolated function between the measured data points for one sensor

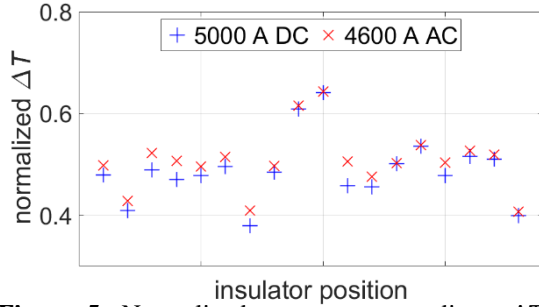


**Figure 5:** Normalized temperature gradients  $\Delta T$  across the insulators

shows the calculation at the sensor position  $i$  with the maximum  $\Delta T$ . The curve  $\Delta T_{i, \text{interpol}}(I_{AC})$  in Figure 4 is nonlinear. In the range of (4000...5000) A the relation  $\Delta T \sim I_{AC}^2$  delivers comparable results as the spline function  $\Delta T_{i, \text{interpol}}(I_{AC})$ . This method is used at all sensor points to get the overall numeric matrix  $\Delta T_{\text{interpol}}(I_{AC})$ . Thereby the temperature gradient at all sensor positions is calculated for a given current  $I_{AC}$ . This current  $I_{AC}$  can then iteratively be increased until all data points for  $\Delta T_{\text{interpol}}$  are equal or higher than  $\Delta T(5000 \text{ A DC})$ . This procedure results in a test current of  $I_{AC \text{ repr.}} = 4594 \text{ A AC}$ , i.e. approx. 4600 A AC. Figure 5 shows the temperature gradient of this representative AC current and the measured temperature gradient at 5000 A rated DC current for the insulator positions. It can be seen, that for every position, the following relation is valid:  $\Delta T(4600 \text{ A AC}) \geq \Delta T(5000 \text{ A DC})$ . For the maximum values, the data points of both currents fit very well, while for the lower values the differences between AC and DC are higher.

### 3.3. TEST CURRENT CALCULATION FOR $\theta$ AT THE INNER CONDUCTOR

Similar to section 3.2., the interpolation curve  $\theta_{\text{interpol}}$  for the temperature-rise  $\theta$  at the inner conductor is evaluated.  $I_{AC \text{ repr.}}$  is increased until the interpolation  $\theta_{\text{interpol}}(I_{AC})$  leads to equal or higher  $\theta$  than for 5000 A DC. It can also be found a relation close to  $\theta \sim I^2$  in the range of (4000...5000) A. The representative AC test current was determined with  $I_{AC \text{ repr.}} = 4560 \text{ A AC}$ , which is approximately 1% lower than the test current considering the temperature gradient at the insulators (see section 3.2).

Both requirements with respect to temperature gradient and temperature-rise would therefore be covered by a representative test current of 4600 A AC. The resulting normalized  $\theta$  for the 20 hottest sensor positions are shown in Figure 6. The following relation is valid for all sensor positions:  $\theta(4600 \text{ A AC}) \geq \theta(5000 \text{ A DC})$ .

Similar calculations can be performed for the less relevant parameters  $\theta$  of the enclosure and  $\Delta T$  of the gas gaps. The test current of 4600 A AC would also result in equal or higher  $\theta$  values at the enclosure. 85% of the  $\Delta T$  values across the gas gap would also be equivalent or higher. Especially all high  $\Delta T$  values for the gas gap would be covered. The remaining 15% are considered as uncritical, because their values are comparably low, e.g. in average 34 % lower than the maximum value.

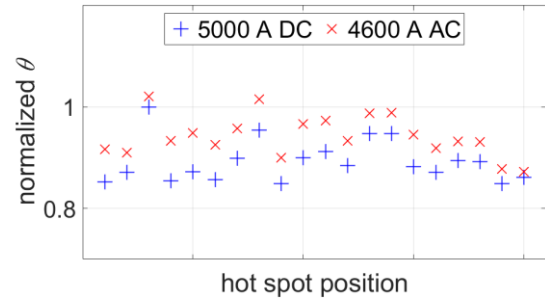


**Figure 6:** Normalized temperature rises  $\theta$  at the 20 hottest sensors at the inner conductor

### 3.4. TEST CURRENT CALCULATION ACCORDING TO IEC/IEEE 65700-19-03

The procedure in section 3.2. and 3.3. is quite time consuming and requires long testing time and mathematical comparisons. A more comfortable process would be desirable. IEC/IEEE 65700-19-03 [17], which is applicable for HVDC bushings, offers a test current calculation  $I_{AC \text{ repr.}}$  based on the ohmic resistance under AC and DC and the rated DC current  $I_{r \text{ DC}}$  of the equipment. The calculation is

based on the assumption of equal power losses for AC and DC current, i.e.  $P_{AC} = P_{DC}$  (refer equation (2)).<sup>3</sup>

$$I_{AC \text{ repr.}} = I_{r \text{ DC}} \cdot \sqrt{\frac{R_{DC}(T_{HL})}{R_{AC}(T_{HL})}} \quad (2)$$

IEC/IEEE 65700-19-03 [17] considers a measurement of the resistance at high load condition  $T_{HL}$ . Equation (2) can be applied to the test object in Figure 1. The DC resistance  $R_{DC}(20 \text{ }^\circ\text{C})$  of the inner conductor at  $20 \text{ }^\circ\text{C}$  was measured before and after the temperature-rise test. The measurement of the AC resistance  $R_{AC}$  is challenging [18]. For the measurement, the ohmic voltage drop has to be separated from the inductive voltage drop. Since the inductive voltage drop is much higher than the ohmic one, the power angle is nearly  $90^\circ$ . Slight changes of the power angles due to e.g. asymmetric cable lengths across the measuring terminals will highly influence the measurement. Another challenge is the inductive coupling inside the measuring loop. As an easier approach, the value for  $R_{AC}$  is calculated for the considered GIS test assembly in Figure 1.

The inner conductor of the HVDC GIS is made of aluminum of resistivity  $\rho_{Al}$ . By use of the cross section of the average hollow inner GIS conductor  $A$  and its length  $l$  the resistance can be divided into the value for the bulk material and the contact surfaces according to equation (3).

$$R_{DC} = R_{DC, \text{solid}} + R_{DC, \text{contact}} = \rho_{Al} \cdot \frac{l}{A} + R_{DC, \text{contact}} \quad (3)$$

The contact resistance is assumed to be independent from the skin effect. It is further assumed that the AC contact resistance  $R_{AC, \text{contact}}$  is equal to  $R_{DC, \text{contact}}$ . The influence of the skin effect and the corresponding skin factor  $r_{\text{skin}}$  for the bulk material can easily be calculated with the known conductor geometry. With these data,  $R_{AC}$  can be calculated according to equation (4).

$$R_{AC} = R_{AC, \text{solid}} + R_{AC, \text{contact}} = R_{DC, \text{solid}} \cdot r_{\text{skin}} + R_{DC, \text{contact}} \quad (4)$$

The resistances of the contact surfaces, as well as those of the bulk material are temperature dependent [19]. The temperature dependence of the solid material can be well described by application of known material dependent temperature coefficients. In a first approximation it is assumed that this temperature function  $f(T)$  is valid for both parts of the resistivity. Equation (5) shows the overall result based on equation (2):

$$I_{AC \text{ repr}} = I_{r \text{ DC}} \cdot \sqrt{\frac{R_{DC}(20 \text{ }^\circ\text{C}) \cdot f(T)}{R_{AC}(20 \text{ }^\circ\text{C}) \cdot f(T)}} = I_{r \text{ DC}} \cdot \sqrt{\frac{R_{DC}(20 \text{ }^\circ\text{C})}{R_{AC}(20 \text{ }^\circ\text{C})}} = 4610 \text{ A AC} \quad (5)$$

The calculated test current fits well to the determined test current of 4600 A AC according to the iterative interpolation method, presented in section 3.2. and 3.3.

Even when assuming no temperature dependence of the contact surface resistance, the result is changed by only less than 1%. It is assumed that the influence of the temperature dependence for AC and DC is mostly canceling out each other for gas-insulated DC systems.

An even more practical approach according to equation (6) could be used. Due to the good fitting of the calculated test current in section 3.2 and 3.3 it is assumed that it might be sufficient to consider the resistivity at ambient temperature  $T_{\text{amb}}$  according to equation (6).

$$I_{AC \text{ repr}} = I_{r \text{ DC}} \cdot \sqrt{\frac{R_{DC}(T_{\text{amb}})}{R_{AC}(T_{\text{amb}})}} \quad (6)$$

Equation (6) offers the possibility to determine the AC test current of a thermo-electric test assembly by just measuring the AC and DC resistivity at ambient temperature. Then no further temperature-rise tests are required for determining the relation between an AC test current and the rated DC current.

<sup>3</sup> IEC/IEEE 65700-19-03 requires further increase of the test current in order to compensate heating effects from harmonics in the DC current during operation in the DC grid. This influence is neglected in this paper.

## 4. CONCLUSION

Thermo-electric tests on HVDC equipment may utilize conductor heating with an alternating current, since it is easier to inject and to handle than a direct current. To be in line with the recommendations of CIGRE JWG D1/B3.57 [1], a representative AC test current has to be determined for reaching at least the same temperature gradient across the insulators and temperature-rise at the inner conductor than with the rated DC current. Both parameters have the highest impact on the withstand voltage during thermo-electric testing. Thus, the test current should result in similar or higher stresses as they would appear in practice.

The AC test current was determined with temperature-rise tests at a commercial HVDC GIS assembly, which contained all major modules. By interpolation of the test results of different current values, a test current of 4600 A AC was determined to be representative for 5000 A DC. It was shown that the test current results in equal or higher thermal stresses at all sensor positions, except for some uncritical temperature gradients at the gas gaps with slightly lower temperature gradients to the enclosure.

The practical effort for test current evaluation may be reduced by assuming equal power losses for AC and DC current supply (IEC/IEEE 65700-19-03 [17]). Based on the available data, this approach results in the same test current of approximately 4600 A AC. The paper shows that the equal power loss approach is applicable in practice for gas-insulated systems, since the calculated test current is equal to the value based on the temperature-rise tests. As expected, temperature-rise is proportional to  $I^2$  and thereby to the power losses, which also explains the well coincidence of both approaches. It is assumed that this relation is valid for other types of gas-insulated systems as well. Furthermore, the calculation with equal power losses could further be reduced to measurements or calculations of the DC and AC resistance at ambient temperature, because the temperature dependency of AC and DC resistance will nearly cancel each other out.

The AC test current for thermo-electric tests was finally decided to be set to 4700 A AC in order to thermally represent 5000 A DC [9]. This decision includes some safety margins, the heating influence of current harmonics in the grid and covers potential fluctuation of the infeed during testing.

## 5. ACKNOWLEDGMENTS

The authors gratefully acknowledge the substantial support of this work by the IWB-EFRE-Program by the State of Hessen (Funding Code 20002558) and the Bavarian Ministry of Economic Affairs, Regional Development and Energy (Funding Code IET-1208-0018).



Gefördert durch



Bayerisches Staatsministerium für  
Wirtschaft und Medien, Energie  
und Technologie

## BIBLIOGRAPHY

- [1] CIGRE Joint Working Group D1/B3.57: Dielectric testing of gas-insulated HVDC systems. *Technical Brochure to be published*.
- [2] M. Hallas, T. Wietoska, V. Hinrichsen: "Construction of a DC Current Injection Generator for HVDC Long-term Tests up to 5000 A DC at 660 kV DC Potential" In: 21st International Symposium on High Voltage Engineering (ISH), Budapest, Hungary, 26-30 August 2019
- [3] B. M. Weedy: "DC conductivity of voltalit epoxy spacers in SF<sub>6</sub>" In: IEE Proceedings A – Physical Science, Measurement and Instrumentation, Management and Education, Reviews, Volume 132 (Edition 7): pp. 450–454, 1985
- [4] K. Juhre, B. Lutz, D. Imamovic, "Testing and long term performance of gas-insulated DC compact switchgear," CIGRE SC D1 Colloquium, Rio de Janeiro, 2015.
- [5] U. Riechert, M. Salzer, M. Callavik, P. Bergelin, "Compact high voltage direct current (HVDC) transmission systems," Stuttgarter Hochspannungssymposium, Stuttgart 2016.
- [6] Winter, A.; Kindersberger, J.: Transient field distribution in gas-solid insulation systems under DC voltages. IEEE Dielectr. Electr. Insul., vol. 21, pp. 1116-128, 2014.
- [7] Gremaud, R.; Doiron, C.; Baur, M.; Simka, P.; Teppati, V.; Källstrand, B.; Johansson, K.; Hering, M.; Speck, J.; Großmann, S.; Riechert, U.; Straumann, U.: Solid-gas insulation in HVDC gas-insulated system: Measurement, modeling and experimental validation for reliable operation. CIGRÉ-Session, Paris 2016.

- [8] Hering, M.; Speck, J.; Großmann, S.; Riechert, U.: Field transition in gas-insulated HVDC systems. *IEEE Dielectr. Electr. Insul.*, vol. 24, no. 3, pp. 1608-1616, 2017.
- [9] K. Juhre, M. Hering: "Testing and long-term performance of gas-insulated systems for DC application" Paper 10-4, Cigré-IEC 2019 Conference on EHV and UHV (AC & DC), Hakodate, Japan, 23-26 April 2019
- [10] K.-C. Kao: "Dielectric phenomena in solids". San Diego: Elsevier Academic Press, 2004
- [11] T. Wendel, J. Kindersberger, M. Hering, K. Juhre: "Einflussfaktoren auf die Raumladungsdichteverteilung in Epoxidharzformstoff" (in German). In: 1. Fachtagung Polymere Isolierstoffe und ihre Grenzflächen, pages 105–109, Zittau, Germany, 2018
- [12] M. Hering, J. Speck, K. Backhaus, S. Gromann, U. Riechert. Capacitive-resistive transition in gas insulated DC systems under the influence of particles on the insulator surface. 19<sup>th</sup> International Symposium on High Voltage Engineering, Pilsen, August 2015.
- [13] C. Neumann, K. Juhre, U. Riechert, U. Schichler: "Basic phenomena in gas-insulated HVDC systems and adequate dielectric testing" Paper 10-5, Cigré-IEC 2019 Conference on EHV and UHV (AC & DC), Hakodate, Japan, 23-26 April 2019
- [14] L. Iwanow: "Einfluß der Elektrodotemperatur auf die Durchschlagspannung koaxialer SF6-Isolierungen". (in German), PhD thesis, Technical University of Dresden, 1988
- [15] M. Hering, J. Speck, S. Großmann and U. Riechert, "Influence of gas temperature on the breakdown voltage in gas-insulated systems," in *IEEE Transactions on Dielectrics and Electrical Insulation*, vol. 24, no. 1, pp. 401-408, Feb. 2017.
- [16] IEC 62271-203: "High-voltage switchgear and controlgear - Part 203: Gas-insulated metal-enclosed switchgear for rated voltages above 52 kV" Edition 2.0, 2011
- [17] IEC/IEEE 65700-19-03: "Bushings for DC application", Edition 1.0, 2014
- [18] R. Suchantke: "Die Messung von Wechselstromverlusten von Hochspannungskabeln mit großen Querschnitten unter Verwendung der elektrischen Methode" (in German), PhD thesis, Technical University of Dresden, 2018
- [19] C. Ruppert, M. Runde: "Thermally Induced Mechanical Degradation of Contact Spots in Aluminum Interfaces" In: *IEEE Transactions on Components and Packaging Technologies*, volume 29, issue 4, 2006